

Interplay between the kinesin and tubulin mechanochemical cycles underlies microtubule tip tracking by the non-motile ciliary kinesin Kif7

Shuo Jiang^{1,2,*}, Nandini Mani^{1,2,*}, Elizabeth M. Wilson-Kubalek^{3,*}, Pei-I Ku^{1,2}, Ronald A. Milligan³, Radhika Subramanian^{1,2,±}

¹Department of Molecular Biology, Massachusetts General Hospital, Boston, MA 02114, USA

²Department of Genetics, Harvard Medical School, Boston, MA 02115, USA

³The Scripps Research Institute, La Jolla, CA 92037, USA

*Equal contribution

±Corresponding Author

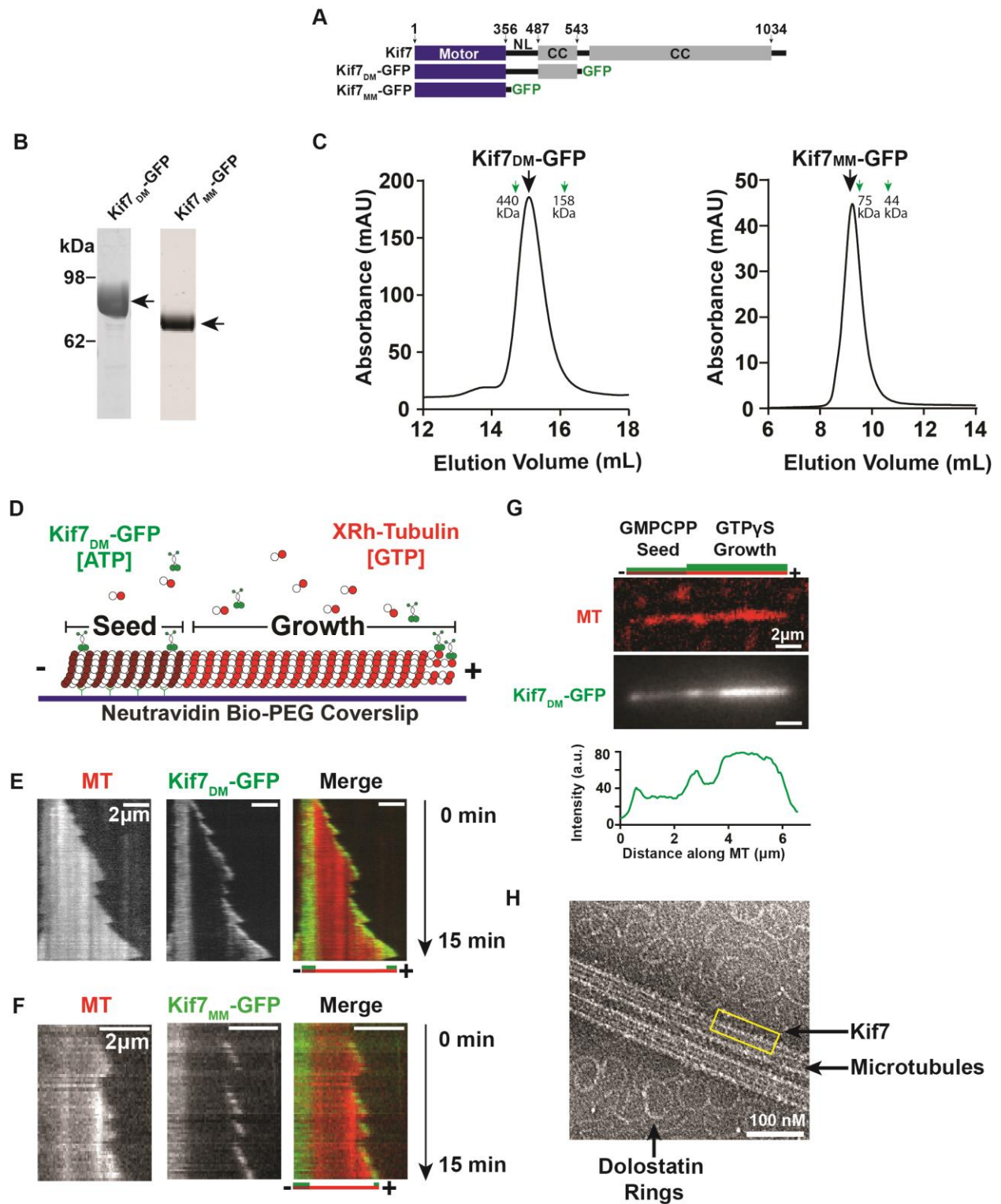


Figure S1

2
3
4

5 **Figure S1.** *Related to Figure 1*

6 **A.** Domain organization indicating the motor domain, neck-linker (NL) and coiled-coil (CC)
7 of full length Kif7 and the constructs used for fluorescence microscopy assays.

8 **B.** SDS-PAGE analysis of purified Kif7_{DM}-GFP (left) and Kif7_{MM}-GFP (right). Arrows as
9 indicators.

10 **C.** Chromatograms from size exclusion chromatography for Kif7_{DM}-GFP (left) (Superose
11 6 increase 10/300 GL) and Kif7_{MM}-GFP (right) (Superdex 75 10/300 GL). Green arrows
12 indicate elution volume of molecular weight markers.

13 **D.** Schematic of the dynamic microtubule assay used to examine Kif7_{DM}-GFP localization
14 on growing microtubules. X-rhodamine-labeled GMPCPP-stabilized microtubule 'seeds'
15 (brown) were immobilized on a glass coverslip via a neutravidin-biotin linkage. Kif7
16 localization on the dynamic microtubule was examined by incubating the seeds with X-
17 rhodamine-labeled tubulin (red), 1 mM GTP, Kif7_{DM}-GFP (green) and 1 mM ATP.

18 **E.** Representative kymograph of the microtubule, GFP and merged channels showing
19 Kif7_{DM}-GFP localization at the tip of the growing microtubule over 15 minutes. The
20 schematic below the image indicates the position of the seed (brown), growth (red) and
21 the associated Kif7_{DM}-GFP signal (green).

22 **F.** Representative kymographs of the microtubule, GFP and merged channels showing
23 Kif7_{MM}-GFP localization at the tip of the growing microtubule over 15 minutes. The
24 schematic below the image indicates the position of the seed (brown), growth (red) and
25 the associated Kif7_{MM}-GFP signal (green).

26 **G.** Representative image of microtubule (top) and associated Kif7_{DM}-GFP (middle) and
27 line scan of Kif7_{DM}-GFP intensity (bottom) obtained from the experiment described in

28 “Figure 1A’. Assay conditions: 150 nM Kif7_{DM}-GFP and 1 mM ATP and 1 mM GTPγS.
29 Microtubule grown only from X-rhodamine labeled tubulin for control. The schematic
30 above the image indicates the position of the seed (brown), GTPγS growth (red) and the
31 associated Kif7_{DM}-GFP signal (green).
32 **H.** Electron micrographs of negatively stained Kif7_{DM}-GFP binding to straight microtubule
33 and dolostatin induced microtubule rings.

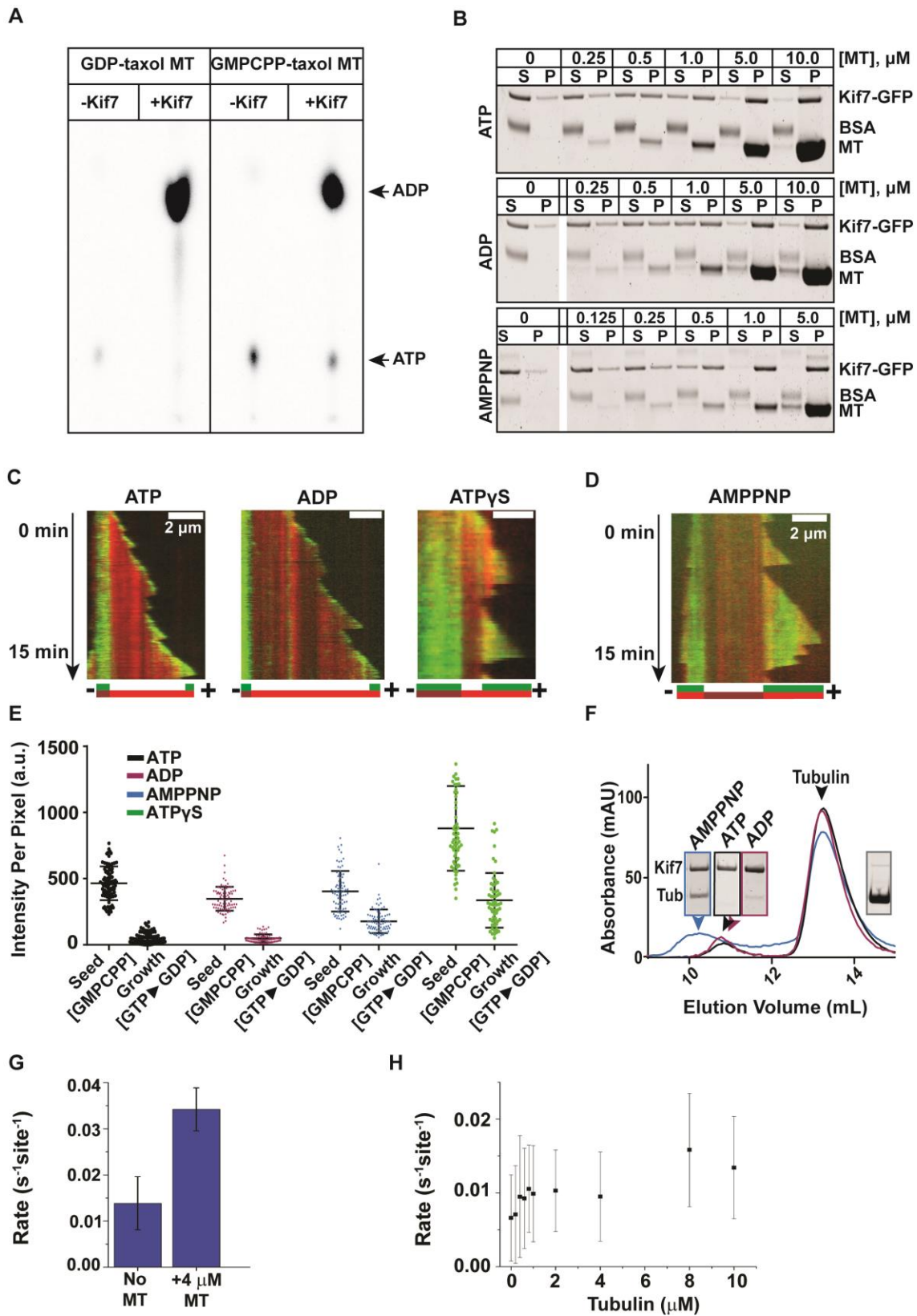


Figure S2

34

35

36 **Figure S2.** *Related to Figure 2*

37 **A.** TLC analysis of the adenosine nucleotide content of Kif7 bound to GMPCPP and GTP
38 polymerized taxol stabilized microtubules. >95% of Kif7 associated is in the ADP form.

39 **B.** SDS-PAGE analysis of Kif7_{DM}-GFP cosedimentation on GDP-taxol stabilized
40 microtubules (0 – 10 μ M) in the presence of 1 mM ATP, ADP and AMPPNP. (S:
41 Supernatant, unbound fraction. P: Pellet, bound fraction. BSA: Bovine Serum Albumin,
42 gel loading control).

43 **C.** Representative kymographs of Kif7_{DM}-GFP localization at the tip of the growing
44 microtubule in the presence of 1 mM ATP, ADP and ATP γ S. The schematic under the
45 image indicates the position of the seed (brown), growth (red) and the associated Kif7_{DM}-
46 GFP signal (green).

47 **D.** Representative merged kymograph showing Kif7_{DM}-GFP localization on the growing
48 microtubule in the presence of AMPPNP. The schematic under the image indicates the
49 position of the seed (brown), growth (red) and the associated Kif7_{DM}-GFP signal (green).

50 **E.** Scatter plot of GFP fluorescence intensity per pixel of Kif7_{DM}-GFP on the GMPCPP-
51 seed and GTP \blacktriangleright GDP growth regions in the presence of different adenosine nucleotides.
52 Error bars represent standard deviation. Assays were performed under Kif7_{DM}-GFP
53 concentrations that resulted in similar average fluorescence intensities on the GMPCPP-
54 seeds in the presence of different nucleotides to allow for normalization. Assay conditions:
55 150 nM Kif7_{DM}-GFP and 1 mM ATP; 250 nM Kif7_{DM}-GFP and 1 mM ADP; 10 nM Kif7_{DM}-
56 GFP and 1 mM AMPPNP; 50 nM Kif7_{DM}-GFP and 1 mM ATP γ S. (GMPCPP-seed: ATP:
57 464.7 ± 127.8 ; N = 81, ADP: 347.2 ± 90.7 ; N = 78, AMPPNP: 403.6 ± 153.1 ; N = 78 and

58 ATP γ S: 879.2 ± 320 ; N = 61. GDP growth: ATP: 49.9 ± 41.3 ; N = 81, ADP: 48.0 ± 30.3 ;
59 N = 78, AMPPNP: 177.4 ± 89.1 ; N = 78 and ATP γ S: 335.9 ± 206.0 ; N = 61).

60 **F.** Size exclusion chromatography (Superdex 200 increase 10/300 GL) and SDS-PAGE
61 analysis (Inset, ATP: black, ADP: purple and AMPPNP: blue) to examine the interaction
62 of Kif7_{DM}-GFP (1 μ M) with free-tubulin dimer (20 μ M) in the presence of 1 mM ATP, ADP
63 and AMPPNP.

64 **G.** ATPase assay showing 3-fold enhancement of Kif7 intrinsic ATPase rate in the
65 presence of microtubules. (No microtubule: $0.014 \pm 0.006 \text{ s}^{-1}\text{site}^{-1}$ and +4 μ M Microtubule:
66 $0.03 \pm 0.005 \text{ s}^{-1}\text{site}^{-1}$).

67 **H.** ATPase assay showing no simulation of the basal ATPase rate of Kif7 by soluble
68 tubulin.

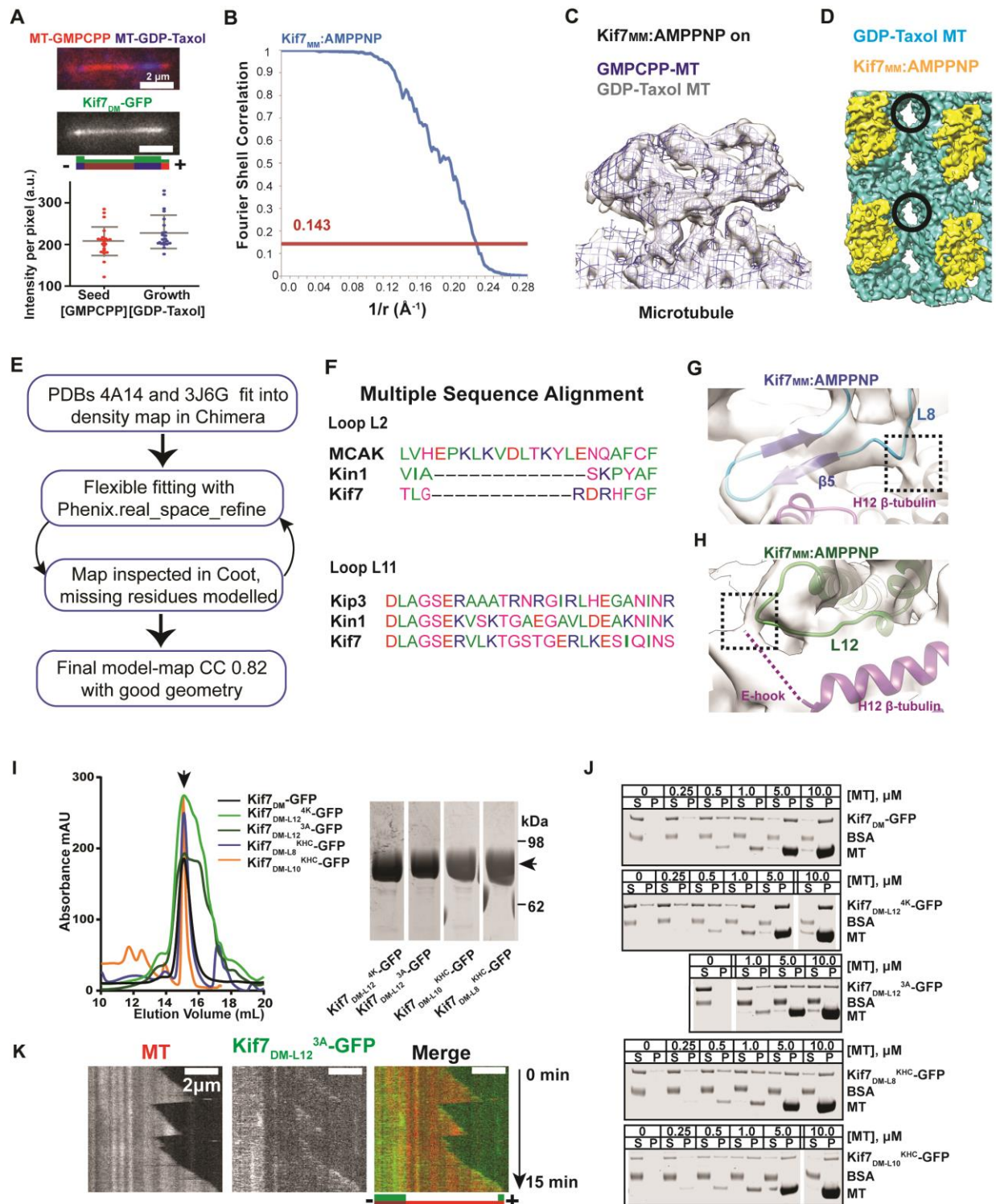


Figure S3

69

70

71

72 **Figure S3.** *Related to Figure 3*

73 **A.** Representative fluorescence image (top) and intensity analysis (bottom) of Kif7_{DM}-GFP
74 associated on segmented microtubules containing a GDP-taxol stabilized growth region
75 (blue). Assay conditions: 150 nM Kif7_{DM}-GFP and 1 mM ATP and 1 mM GDP-taxol. The
76 schematic below the fluorescence image indicates the position of the seed (brown),
77 growth (blue), cap (red) and the associated Kif7_{DM}-GFP signal (green). (GMPCPP-seed:
78 206.9 ± 36.4 ; N = 21. GDP-Taxol growth: 229.3 ± 41.1 ; N=21).

79 **B.** FSC curve for Kif7_{MM}:AMPPNP on GDP-taxol microtubules.

80 **C.** Superposition of cryo-EM reconstructions of Kif7_{MM}:AMPPNP bound to GDP-Taxol
81 stabilized microtubules (gray solid) and GMPCPP-microtubules (blue mesh)

82 **D.** Electron density of Kif7_{MM} (yellow) in complex with AMPPNP, bound on the GDP-taxol
83 microtubule lattice (blue). Circle shows the canonical EB1 binding site in the inter-
84 protofilament region.

85 **E.** Schematic of the procedure for model building and fitting into the EM reconstruction.
86 The initial models used were PDB 4A14: crystal structure of the Kif7 motor domain and
87 PDB 3J6G: EM-derived structure of α - and β -tubulin from GDP-taxol stabilized
88 microtubule.

89 **F.** Multiple sequence alignment of Loops L2 and L11 in Kif7 with other kinesins. The
90 structure-based sequence alignment of L2 between MCAK, Kinesin-1 and Kif7 (PDB IDs:
91 4UBF, 1BG2 and 4A14, respectively), and the sequence alignment of L11 between Kip3,
92 Kinesin-1 and Kif7 (Uniprot IDs: P53086, P33176, Q2M1P5) are shown.

93 **G. & H.** Enlarged view of structural elements of Kif7_{MM}:AMPPNP with insertions in
94 sequence compared to Kin1:ATP. Helix H12 and E-hook (dotted line) of β -tubulin are

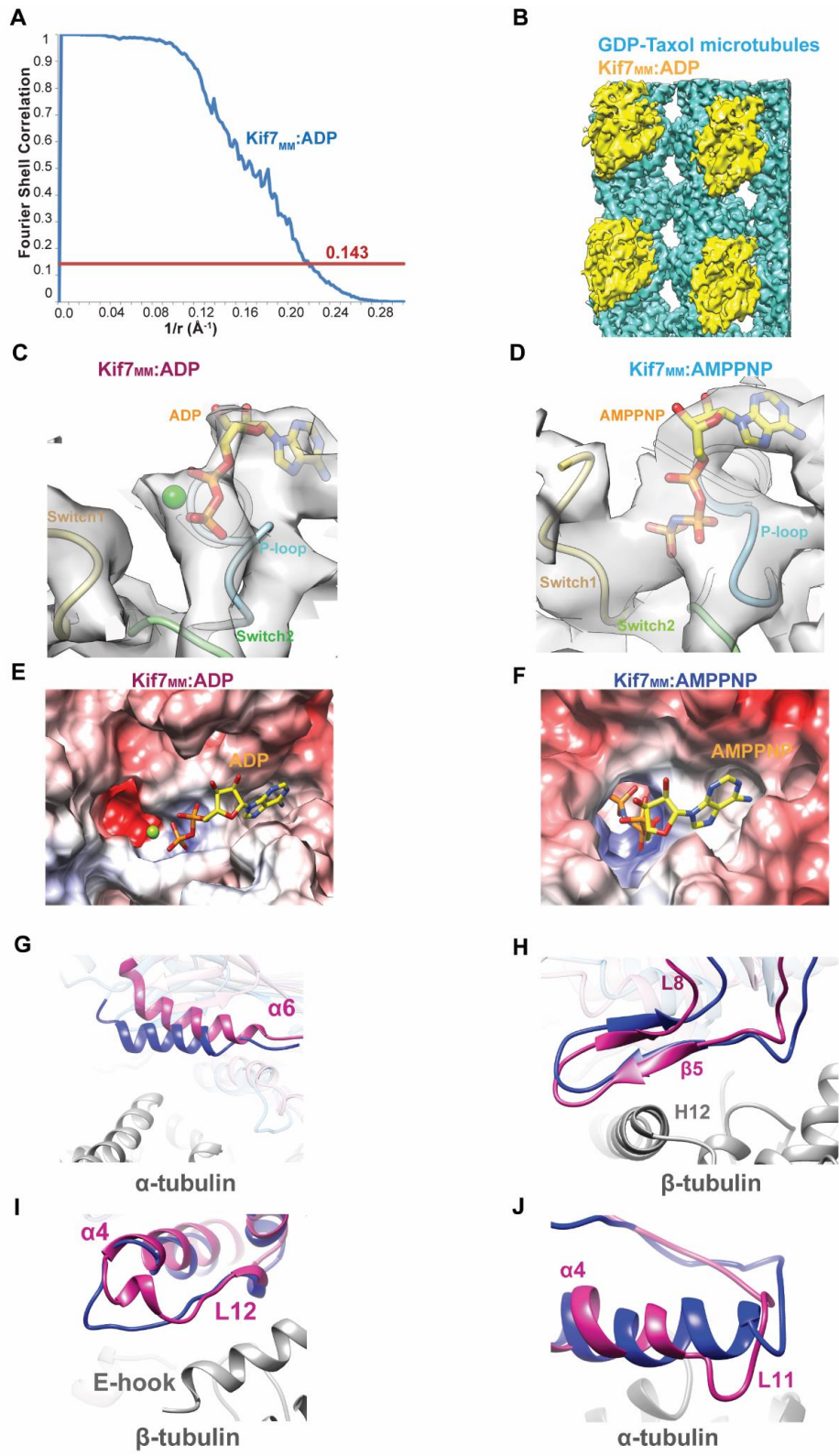
95 shown in purple. The black boxes highlight the insertions in **(F)** Loop L8-strand β 5 (blue)
96 of Kif7_{MM}:AMPPNP **(G)** Helix α 4 and loop L12 (green) of Kif7_{MM}:AMPPNP.

97 **I.** Purification of all Kif7_{DM}-GFP mutant constructs used in the microtubule co-
98 sedimentation assays. Size exclusion chromatograms (left) of constructs: Kif7_{DM}-GFP
99 (black), Kif7_{DM-L12}^{4K}-GFP (light green), Kif7_{DM-L12}^{3A}-GFP (dark green), Kif7_{DM-L8}^{KHC}-GFP
100 (blue) and Kif7_{DM-L10}^{KHC}-GFP (orange) through a Superose 6 increase 10/300 GL column.
101 Arrow indicates Kif7 elution peak. SDS-PAGE of purified proteins is shown on the right.

102 **J.** SDS-PAGE analysis of cosedimentation experiments of Kif7_{DM}-GFP mutants on GDP-
103 taxol stabilized microtubules in the presence of 1 mM ATP. (S: Supernatant, unbound
104 fraction. P: Pellet, bound fraction. BSA: Bovine Serum Albumin, gel loading control).

105 **K.** Representative kymograph of the microtubule, GFP and merged channels showing
106 Kif7_{DM-L12}^{3A}-GFP localization at the tip of the growing microtubule in the presence of ATP.
107 The schematic under the image indicates the position of the seed (brown), growth (red)
108 and the associated Kif7_{DM-L12}^{3A}-GFP signal (green).

109
110



111

112

113

Figure S4

114 **Figure S4.** *Related to Figure 4*

115 **A.** FSC curve for Kif7_{MM}:ADP on GDP-taxol microtubules.

116 **B.** Electron density of Kif7_{MM} (yellow) in complex with ADP, bound on the GDP-taxol
117 microtubule lattice (blue).

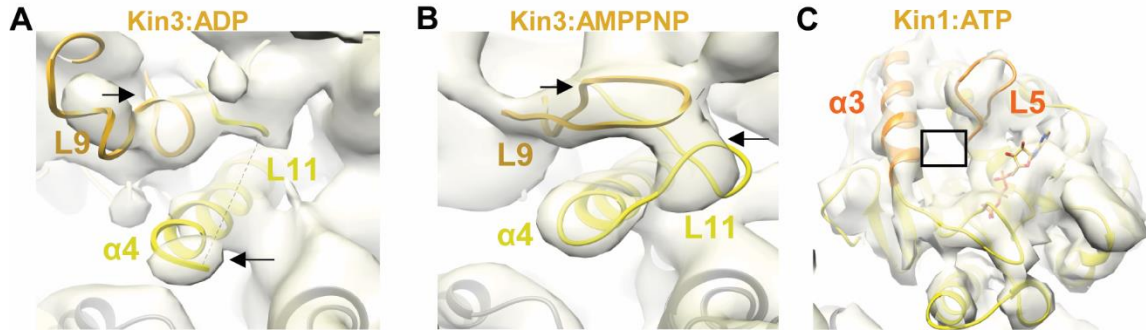
118 **C&D.** Enlarged view of the NBP for **(C)** Kif7_{MM}:ADP and **(D)** Kif7_{MM}:AMPPNP. Nucleotides
119 are rendered as yellow sticks. Structural elements flanking the NBP are Switch1 (khaki),
120 Switch2 (green) and P-loop (light blue).

121 **E&F.** Electrostatic surface representation of the NBP in **(E)** Kif7_{MM}:ADP and **(F)**
122 Kif7_{MM}:AMPPNP. Nucleotides are rendered as yellow sticks. Surface potential ranges
123 from -7 (red) to +7 (blue) KT/e.

124 **G-J.** Enlarged views showing the superposition between the different secondary structure
125 elements in Kif7_{MM}:AMPPNP (blue) and Kif7_{MM}:ADP (pink). **(G)** Helix α_6 , **(H)** Loop L8 and
126 strand β_5 . **(I)** Helix α_4 and loop L12. **(J)** Helix α_4 and loop L11 of Kif7. α - and β -tubulin
127 are shown as gray ribbons.

128

129



130

131

132

Figure S5

133 **Figure S5.** *Related to Figure 5*

134 **A&B.** Enlarged views of the pincer-like movement of loops L9 and L11 during the ADP to
135 AMPPNP transition in Kinesin-3 (Kin3). **(A)** Kin3:ADP (PDB:4UXS, EMD: 2768), **(B)**
136 Kin3:AMPPNP (PDB:4UXP, EMD: 2766). Arrows highlight the movement of loops L9 and
137 L11.

138 **C.** Enlarged view of the α 3 and L5 region in Kin1:ATP (PDB:3J8Y, EMD: 6188). Black
139 box highlights the absence of density connecting α 3 and L5.

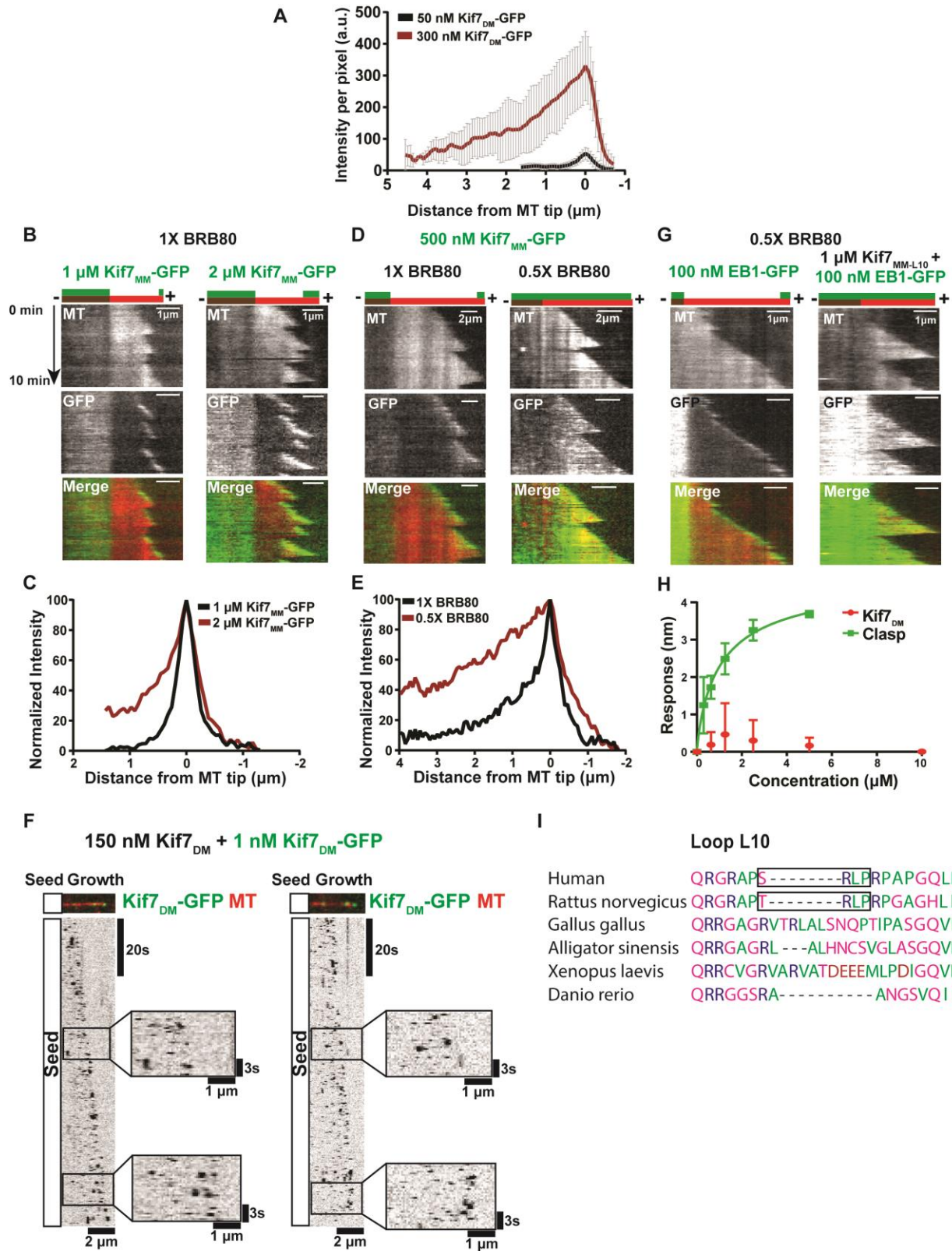


Figure S6

140

141

142

143 **Figure S6.** *Related to Figure 6*

144 **A.** Averaged GFP fluorescence intensity profile of Kif7_{DM}-GFP along the growing
145 microtubule-ends at 50 nM (black; N=25) and 300 nM (brown, N=25). Error bars represent
146 standard deviation.

147 **B.** Representative kymograph of the microtubule, GFP and merged channels showing
148 Kif7_{MM}-GFP localization on the growing microtubule at 1 μ M and 2 μ M concentrations.
149 The schematic above the image indicates the position of the seed (brown), growth (red)
150 and the associated Kif7_{MM}-GFP signal (green).

151 **C.** Normalized GFP fluorescence intensity profile of Kif7_{MM}-GFP along the growing
152 microtubule-ends at 1 μ M (black; N=20) and 2 μ M (brown, N=20) concentrations.

153 **D.** Representative kymograph of the microtubule, GFP and merged channels showing
154 500 nM Kif7_{MM}-GFP localization on the growing microtubule at 1X BRB80 and 0.5X
155 BRB80. The schematic above the image indicates the position of the seed (brown),
156 growth (red) and the associated Kif7_{MM}-GFP signal (green).

157 **E.** Normalized GFP fluorescence intensity profile of 500 nM Kif7_{MM}-GFP along the
158 growing microtubule-ends at 1X BRB80 (black; N=20) and 0.5X BRB80 (brown, N=20).

159 **F.** Snapshot of spiked single-molecule tracking experiment during Kif7 expansion on the
160 growing microtubule lattice. 1 nM Kif7_{DM}-GFP (green) and 150 nM Kif7_{DM} on growing X-
161 rhodamine labeled microtubules (red) at 150 nM concentrations where expansion is
162 visible (top). Representative kymograph generated from the microtubule in **(E)** showing
163 the localization of Kif7_{DM}-GFP at microtubule-ends (bottom). Inset shows enlarged
164 regions of the single-molecule tracking.

165 **G.** Representative kymograph of the microtubule, GFP and merged channels showing
166 100 nM EB1-GFP localization on the growing microtubule alone and in the presence of 1

167 μM Kif7_{MM-L10}. The schematic above the image indicates the position of the seed (brown),
168 growth (red) and the associated Kif7_{MM}-GFP signal (green).

169 **H.** Biolayer interferometry assay to quantitatively examine the binding affinity of Kif7_{DM}
170 (red; 0-10 μM) and Clasp (green; 0-5 μM) to EB1. Error bars represent standard deviation.
171 The plots of BLI response of Kif7_{DM} and Clasp bound versus concentration were fit to a
172 Hill equation to determine the equilibrium dissociation constants at different
173 concentrations. (K_d for Kif7_{DM}: No Binding and Clasp: $1.1 \pm 0.3 \mu\text{M}$).

174 **I.** Multiple sequence alignment of loop L10 of vertebrate Kif7 homologues from human,
175 rat (*Rattus norvegicus*), domestic chicken (*Gallus gallus*), Chinese alligator (*Alligator*
176 *sinensis*), *Xenopus laevis* and zebrafish (*Danio Rerio*) [Uniprot IDs: Q2M1P5, D4A9P0,
177 F1P446, A0A1U7SD20, A0A1L8H0X0 and Q58G59, respectively]. [S/T]x[I/L]P motifs are
178 highlighted by a black box.

179

180

181

Table S1-Related to Figures 3 and 4

182

Data collection and reconstruction

183

	Kif7_{MM}:AMPPNP (15 protofilaments)	Kif7_{MM}:AMPPNP (14 protofilaments)	Kif7_{MM}:ADP (15 protofilaments)	Kif7_{MM}:ADP (13 protofilaments)
Data collection				
Microscope	Titan Krios (FEI)	Titan Krios (FEI)	Titan Krios (FEI)	Titan Krios (FEI)
Voltage (kV)	300	300	300	300
Nominal magnification*	22,500X	22,500X	22,500X	22,500X
Cumulative exposure dose (e ⁻ Å ⁻²)	37	37	44	44
Exposure rate (e ⁻ /pixel/sec)	4.7	4.7	4.7	4.7
Detector	K2 Summit	K2 Summit	K2 Summit	K2 Summit
Pixel size (Å)*	1.31	1.31	1.31	1.31
Defocus range (µm)	0.7-4.24	0.7-4.24	0.86-2.91	0.86-2.91
Average defocus (µm)	2.31	2.31	1.6	1.6
Micrographs Used	428	428	697	697
Total extracted helical segment (no.)	79,125	79,125	50,409	50,409
Refined helical segment (no.)	25,402	44,295	15,919	19,035
Reconstruction				
Final helical segments (no.)	25,402	37,220	15,919	13,488
Symmetry imposed	HP	HP	HP	HP
Resolution (global) FSC 0.143	4.2	4.3	4.2	6.5

184

185

186

Table S2-Related to Figures 3 and 4

187

Atomic model refinement statistics

	Kif7_{MM}:AMPPNP	Kif7_{MM}:ADP
Refinement protocol	Phenix	Phenix
Resolution for refinement	4.3	4.2
RMS bonds (Å)	0.011	0.006
RMS angles (°)	1.37	1.30
All-atoms clashscore	19	14
Rotamer outliers (%)	3	2
Ramachandran allowed (%)	12	10
Ramachandran favored (%)	88	90
Ramachandran outliers (%)	0	0
Model-map real-space correlation coefficient	0.81	0.83

188

189